I. FORMALISM

Non-standard interactions are sub-leading contributions to neutrino flavor transitions arising from neutrino interactions not considered in the Standard Model. We consider matter NSIs arising from the neutral current NSIs, which exclude production and detection effects. An effective four-fermion Lagrangian for this type of interaction can be written as

$$\mathcal{L}_{\text{NC}} = -2\sqrt{2}G_F \epsilon_{\alpha\beta}^{fX} \left(\bar{\nu}_\alpha \gamma^\mu P_L \nu_\beta \right) \left(\bar{f} \gamma_\mu P_X f \right) , \tag{1}$$

where NC denotes the neutral current interaction with $f \in \{e, u, d\}$, and P_X is the chirality projection operators with $X \in \{L, R\}$.

For chirality X, the NSI Hamiltonian takes the form

$$H = \frac{1}{2E} U M^2 U^\dagger + \sqrt{2}G_F n_e \text{diag}(1, 0, 0) + \sqrt{2}G_F \sum_f n_f \epsilon^{fX} \tag{2}$$

We have no independent sensitivity for the chirality of ϵ^{fX}, so we sum over these to obtain the vectorial parameter as $\epsilon_{\alpha\beta}^{fV} = \epsilon_{\alpha\beta}^{fL} + \epsilon_{\alpha\beta}^{fR}$. Moreover, we normalize the fermion number density n_f by the electron number density n_e. Our matter study will be wholly confined to the interior of the Earth, where we assume electrical neutrality and equal distribution of neutrons and protons, so we use the relations $n_u/n_e \simeq n_d/n_e \simeq 3$. The effective NSI parameters in matter now take the form

$$\begin{aligned}
\epsilon_{\alpha\beta} &= \sum_{f,X} \frac{n_f}{n_e} \epsilon_{\alpha\beta}^{fX} \\
&= \epsilon_{\alpha\beta}^{eV} + 3\epsilon_{\alpha\beta}^{uV} + 3\epsilon_{\alpha\beta}^{dV} \tag{3}
\end{aligned}$$

We note that our definition of $\epsilon_{\alpha\beta}$ differs from some texts, where the quark number density is used to normalize the parameters[?].

With the matter potential $V = \sqrt{2}G_F n_e$, we write

$$H = \frac{1}{2E} U M^2 U^\dagger + V \begin{bmatrix} 1 + \epsilon_{ee} & \epsilon_{e\mu} & \epsilon_{e\tau} \\ \epsilon_{e\mu} & \epsilon_{\mu\mu} & \epsilon_{\mu\tau} \\ \epsilon_{e\tau} & \epsilon_{\mu\tau} & \epsilon_{\tau\tau} \end{bmatrix} , \tag{4}$$

where we have assumed the components of the NSI matrix to be real. In Fig. 1, we study the flux ratio arising from the introduction of the NSI parameter $\epsilon_{\mu\tau}$. Fig. 4a shows the difference $P_{\mu\mu}(\epsilon_{\mu\tau} > 0) - P_{\mu\mu}(\epsilon_{\mu\tau} < 0)$ in the low GeV energy range.

II. DETECTOR FORMALISM

The neutrino flux at the detector is calculated by propagating the atmospheric neutrino flux from Honda et al [1] through the Earth by solving the Schrödinger equation for varying density. The Earth density profile is taken from the PREM [2]. The baseline for a given trajectory is determined using an average neutrino production height of 15 km and an Earth radius of 6371 km. The propagation does not include neutrino absorption.

The oscillation probability $P_{\alpha\beta}$ acts as a weight to the atmospheric flux, yielding the propagated flux for flavor β at detector level as

$$\phi_\beta^{\text{det}} = \sum_\alpha P_{\alpha\beta} \phi_\alpha^{\text{atm}} , \tag{5}$$

where we sum over the initial lepton flavors $\alpha \in \{e, \mu, \bar{e}, \bar{\mu}\}$. To illustrate the impact of $\epsilon_{\mu\tau}$ on both probability and flux level, we plot the flux ratios resulting from Eq. 5 in Fig. 1. In the left panel, we have marked the region in which 99% of the DeepCore cascade events originating from ν_e and ν_τ fluxes are contained. In the right panel, we show the two regions in which 99% of the IceCube and DeepCore track events originating from ν_μ fluxes are contained. Starting with the ν_μ flux ratio, we see that the only clear signal discernible to the IceCube detector is a energy-independent flux deficiency with a factor of $\sim \sqrt{10}$ from core-crossing neutrinos within a zenith range of $\cos(\theta_z^{true}) < -0.87$. DeepCore on the other hand, is exposed to multiple fringes of flux surpluses with a factor ~ 10. The strongest surplus at 20 GeV is very weakly zenith dependent, a stark contrast to the energy-independent but zenith-sensitive IceCube deficiency.
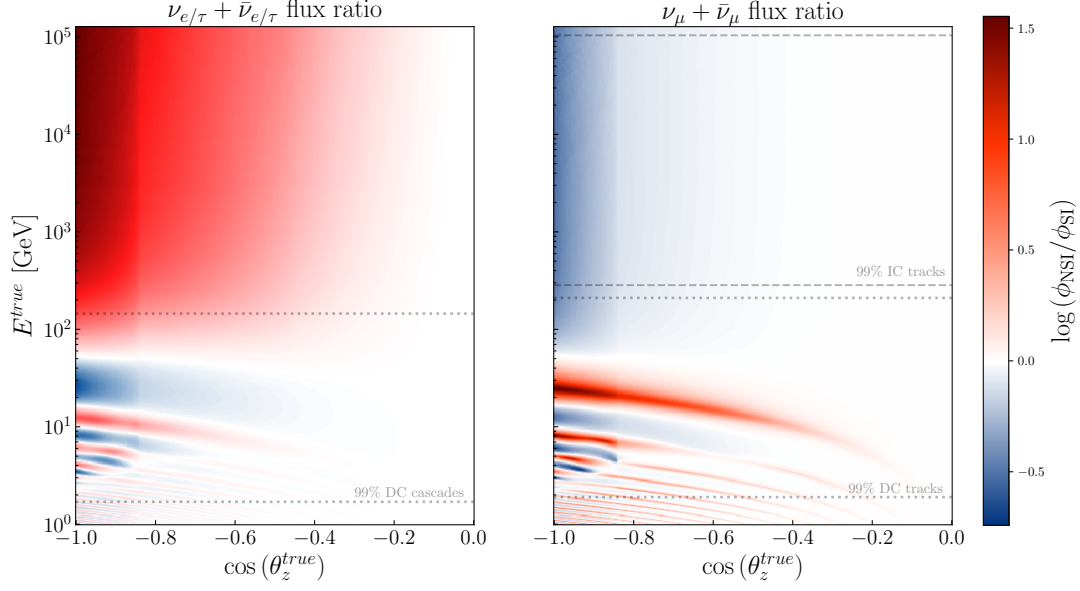
FIG. 1: Ratio of detector NSI to SI atmospheric fluxes. We set $\epsilon_{\mu\tau} = -0.05$, and all other $\epsilon_{\alpha\beta} = 0$. Within the dotted (dashed) boundaries, 99% of the DeepCore (IceCube) MC events are contained. Since we limit our IceCube study to muon tracks, a dashed region is omitted in the left panel.

In IceCube, we will only consider muon track events. Thus, we have to resort to the DeepCore/PINGU detector alone for the ν_e and ν_τ fluxes. Here we see a somewhat weaker signal, this time a zenith-independent deficiency. Where we earlier had surpluses with a factor ~ 10, we now have deficiencies in the order of $\sim \sqrt{10}$.

The muonic flux not only carries the largest $\epsilon_{\mu\tau}$ effect, but it is also more abundant than the ν_e flux. Thus, we expect to receive the highest statistics from μ-related NSI parameters, thus constraining them the strongest. $\epsilon_{\alpha\beta}$ which are only indirectly weakly dependent on the μ channel will have the weakest bounds. This could be improved by considering cascade events in IceCube, thus opening up the e and τ channels there.

A. IceCube

We obtain the data from the IC-86 sterile data release [3], which was collected over 8 years. The event rate for each bin reads

$$N_{ij} = T \sum_\beta \int_{(\cos\theta_z^r)_i}^{(\cos\theta_z^r)_{i+1}} \mathrm{d}\cos\theta_z^r \int_{E_j^r}^{E_{j+1}^r} \mathrm{d}E^r \int_0^\pi R(\theta^r, \theta^t)\mathrm{d}\cos\theta^t \int_0^\infty \phi_\beta^{\mathrm{det}}(E^t, \theta^t) A^{\mathrm{eff}}(E^t) R(E^r, E^t)\mathrm{d}E^t \,, \qquad (6)$$

where T is the live time of the detector, and A^{eff} its effective area averaged over the flavors β from [4]. $R(x^r, x^t)$ is a resolution function, which is responsible for the smearing between the reconstructed and true parameters x^r and x^t, respectively. We assume a log-normal distribution, giving it the form

$$R(x^r, x^t) = \frac{1}{\sqrt{2\pi}\sigma_{x^r} x^r} \exp\left[-\frac{(\log x^r - \mu(x^t))^2}{2\sigma_{x^r}^2}\right] \,. \qquad (7)$$

However, the energy reconstruction is biased, which means that we don't assume that $\mu(E^t) = E^r$ [5]. To model this relationship between E^{true} and E^{reco}, we train a Gaussian process regressor on the IC-86 Monte Carlo [6], from which we can extract a predicted mean and standard deviation for a given E^{reco}. We then take the E^{true} points of the 99th percentile of each distribution to obtain the limits over which to integrate. We take the angular resolution function to be identically unity since the angle resolution in IceCube for track-like events is less than $2°$, making $\cos(\theta_z^{true})$ coincide with $\cos(\theta_z^{reco})$ for our study [3].

B. DeepCore

We use the publically available DeepCore data sample [7] which is an updated version of what was used by the IceCube collaboration in a ν_μ disapprearance analysis [8].

The detector systematics include ice absorption and scattering, as well as overall, lateral, and head-on optical efficiencies of the DOMs. They are applied as correction factors using the best-fit points from the DeepCore 2019 ν_τ appearance analysis [9].

The data include 14901 track-like events and 26001 cascade-like events, both divided into eight $\log_{10} E^{reco} \in [0.75, 1.75]$ bins, and eight $\cos(\theta_z^{reco}) \in [-1, 1]$ bins. Each event has a Monte Carlo weight $w_{ijk,\beta}$ from which we can construct the event count as

$$N_{ijk} = C_{ijk} \sum_\beta w_{ijk,\beta}\, \phi_\beta^{\text{det}}\,, \tag{8}$$

where $C_{k\beta}$ is the correction factor from the detector systematic uncertainty and ϕ_β^{det} is defined as Eq. 5. We have now substituted the effect of the Gaussian smearing by treating the reconstructed and true quantities as a migration matrix.

The oscillation parameters used on our DeepCore simulations are from the best-fit in the global analysis in [10]: $\theta_{12} = 33.44°$, $\theta_{13} = 8.57°$, $\Delta m_{21}^2 = 7.42\,\text{eV}^2$, and we marginalize over Δm_{31}^2 and θ_{23} between their 3σ limits $2.435 \times 10^{-3}\,\text{eV}^2$ to $2.598 \times 10^{-3}\,\text{eV}^2$ and $40.1°$ to $51.7°$, respectively.

C. PINGU

The methodology behind the PINGU simulations is the same as with our DeepCore study II B. We use the public Monte Carlo [11], which allows us to construct the event count as in Eq. 8. However, since no detector systematics is yet modeled for PINGU, the correction factors C_{ijk} are all unity. We will remedy this by including an uncorrelated systematic error. As with the DeepCore Monte Carlo, the PINGU Monte Carlo is divided into eight $\log_{10} E^{reco} \in [0.75, 1.75]$ bins, and eight $\cos(\theta_z^{reco}) \in [-1, 1]$ bins for both track- and cascade-like events. We plot the normalized event differences $(N_{NSI} - N_{SI})/\sqrt{N_{SI}}$ for cascades and tracks in Fig. 5. We generate 'data' by predicting the event rates at PINGU with the following best-fit parameters from [10], except for the CP-violating phase which is set to zero for simplicity.

$$\Delta m_{21}^2 = 7.42 \times 10^{-5}\,\text{eV}^2,\;\; \Delta m_{31}^2 = 2.517 \times 10^{-3}\,\text{eV}^2,$$
$$\theta_{12} = 33.44°,\;\;\; \theta_{13} = 8.57°,\;\;\; \theta_{23} = 49.2°,\;\;\; \delta_{\text{CP}} = 0\,. \tag{9}$$

III. RESULTS

In this section, we present the results from the experiments alone, as well as jointly.

A. Methodology

For our analyses, we define our χ^2 as

$$\chi^2(\hat{\theta}, \alpha, \beta, \kappa) = \sum_{ijk} \frac{\left(N^{\text{th}} - N^{\text{data}}\right)_{ijk}^2}{\left(\sigma_{ijk}^{\text{data}}\right)^2 + \left(\sigma_{ijk}^{\text{syst}}\right)^2} + \frac{(1-\alpha)^2}{\sigma_\alpha^2} + \frac{\beta^2}{\sigma_\beta^2} \tag{10}$$

where we minimize over the model parameters $\hat{\theta} \in \{\Delta m_{31}^2, \theta_{23}, \epsilon\}$, the penalty terms α and β, and the free parameter κ. N_{ijk}^{th} is the expected number of events from theory, and N_{ijk}^{data} is the observed number of events in that bin. We set $\sigma_\alpha = 0.25$ as the atmospheric flux normalization error, and $\sigma_\beta = 0.04$ as the zenith angle slope error [1]. The observed event number has an associated Poissonian uncertainty $\sigma_{ijk}^{\text{data}} = \sqrt{N_{ijk}^{\text{data}}}$. For IceCube, the event count takes the form

$$N_{ijk}^{\text{th}} = \alpha\left[1 + \beta(0.5 + \cos(\theta_z^{reco})_i)\right] N_{ijk}(\hat{\theta})\,, \tag{11}$$

Experiment	Worst case	Normal case	Best case
IceCube	15%	10%	5%
PINGU	5%	3%	0%

TABLE I: Definition of the worst and best case scenarios considered in each experiment, modelled by $\sigma_{ijk}^{\text{syst}} = f\sqrt{N_{ijk}^{\text{data}}}$ with f from the table. We do not consider different DeepCore scenarios because her systematic error distribution is already provided in the data release [7].

with $N_{ijk}(\hat{\theta})$ from Eq. 6. Here, we allow the event distribution to rotate around the median zenith angle of $\cos(\theta_z^{reco}) = -0.5$.

For DeepCore and PINGU, and the event count takes the form

$$N_{ijk}^{\text{th}} = \alpha\left[1 + \beta\cos\left(\theta_z^{reco}\right)_i\right]N_{ijk}(\hat{\theta}) + \kappa N_{ijk}^{\mu_{atm}}\,, \tag{12}$$

with $N_{ijk}(\hat{\theta})$ from Eq. 8. $N_{ijk}^{\mu_{atm}}$ is the muon background, which is left to float freely in the DeepCore analysis. The background at PINGU can be considered negligible to first order [11], and we thus put $\kappa = 0$ when calculating the PINGU χ^2. For DeepCore and PINGU, the median zenith angle is $\cos(\theta_z^{reco}) = 0$, we allow the event count to rotate around this point.

We treat the uncorrelated systematic uncertanties differently for each detector. For IceCube, we set $\sigma_{ijk}^{\text{syst}} = f\sqrt{N_{ijk}^{\text{data}}}$. We consider best, normal, and worst-case scenarios in IceCube assuming $f = 5\%$, 7.5%, and $f = 15\%$ respectively. For PINGU, we use the same form but instead assume $f = 0\%$, 3%, and $f = 5\%$. For DeepCore, we use the provided systematic error distribution which accounts for uncertainties in the finite MC statistics and the data-driven muon background estimate [7]. This is summarized in Table I.

B. Constraining the NSI parameters

First, we set all standard oscillation parameters to their current best-fit values of Eq. 9, except for Δm_{31}^2 and θ_{23}, which we marginalize over their 3σ ranges of 2.435×10^{-3} to $2.598 \times 10^{-3}\,\text{eV}^2$ and 40.1 to $51.7°$ respectively. After the oscillation parameters have been marginalized out, we plot $\Delta\chi^2$ for each of the four NSI parameters in Fig. **??**. We record the confidence levels in Table II and Table III, and best-fit points in Table IV.

We see asymmetrical shapes in the $\Delta\chi^2$ plots in Fig. **??**, especially in $\epsilon_{\mu\tau}$ and $\epsilon_{e\tau}$. We investigate this for $\epsilon_{\mu\tau}$ by plotting the muon survival probability difference $P_{\mu\mu}(\epsilon_{\mu\tau}^+) - P_{\mu\mu}(\epsilon_{\mu\tau}^-)$, where $\epsilon_{\mu\tau}^{\pm} = \pm 0.05$ in Fig. 4a. Muon events are the most abundant, and it suffices to study $P_{\mu\mu}$ to explain the $\epsilon_{\mu\tau}$ asymmetry. We see see that positive $\epsilon_{\mu\tau}$ generates a slightly higher $P_{\mu\mu}$ for energies around $20\,\text{GeV}$ (blue area), while negative $\epsilon_{\mu\tau}$ produces higher $P_{\mu\mu}$ for almost all other combinations of $E^{true}, \cos(\theta_z^{true})$. As we see in Fig. 1, this muon survival abundance is indeed preserved at flux level. So the flux for $\epsilon_{\mu\tau} > 0$ is higher than the flux for $\epsilon_{\mu\tau} < 0$. Is this still true at event level, i.e. after reconstruction? As we see in Fig. 4b, the binned PINGU event counts display strong differences for many bins, giving a high $\Delta\chi^2$ on both sides of $\epsilon_{\mu\tau} = 0$ and slightly higher for $\epsilon_{\mu\tau} = -0.01$. DeepCore on the other hand, has fewer bins where the event count for $\epsilon_{\mu\tau} = -0.01$ surpasses the event count for $\epsilon_{\mu\tau} = +0.01$, giving weaker statistics for the negative side. Thus, we conclude that the DeepCore $\epsilon_{\mu\tau}$ asymmetry stems from the lower statistics for $\epsilon_{\mu\tau} < 0$ at probability level, which is then preserved through the flux and finally the reconstruction.

Comparing Fig. 4b with the flux ratios in Fig. 1, we see that the reconstruction of PINGU is superior to DeepCore, since the event ratio $\log(N_{NSI}^+/N_{NSI}^-)$ (which is in reconstructed quantities) more closely matches the flux ratio $\log(\phi_{NSI}/\phi_{SI})$ (which is in true quantities). This is most evident below $20\,\text{GeV}$, where the DeepCore reconstruction has washed out the fringes while PINGU still has the N_{NSI}^- surplus below $10\,\text{GeV}$.

Comparing the PINGU and the DeepCore results in Fig. 2, we note that the best-fit for each NSI parameter for the PINGU experiment is expected to be zero. This is because the 'data' we generated during the PINGU simulations assume no NSI since they have yet to be observed in nature. This introduces a non-NSI bias in all joint analyses which include PINGU, since PINGU has stronger statistics than DeepCore and will thus pull the joint χ^2 towards $\epsilon = 0$.

For the joint analysis, we follow the parameter goodness-of-fit prescription [12] and construct the joint χ^2 as

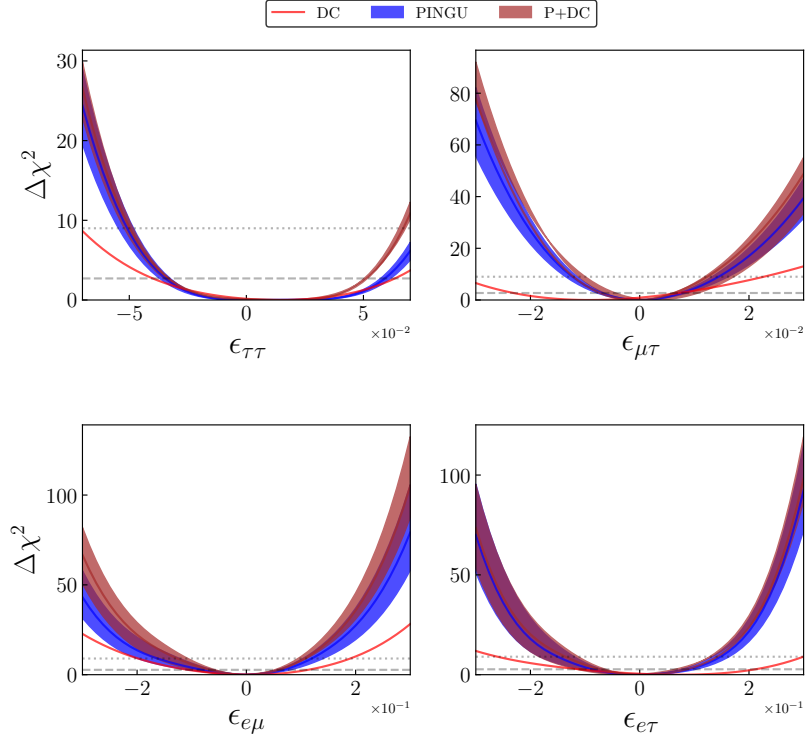$$\chi_{\text{joint}}^2 = \sum_{\text{exp}}\chi_{\text{exp}}^2 - \chi_{\text{exp,min}}^2 \tag{13}$$

FIG. 2: PINGU and DeepCore best-case scenario, with their joint $\Delta\chi^2$ in black. Δm_{31}^2 and θ_{23} and have been marginalized out, and all other NSI parameters other than the one shown are fixed to zero. IceCube tracks only reveal $\epsilon_{\mu\tau}$, and are displayed separately.
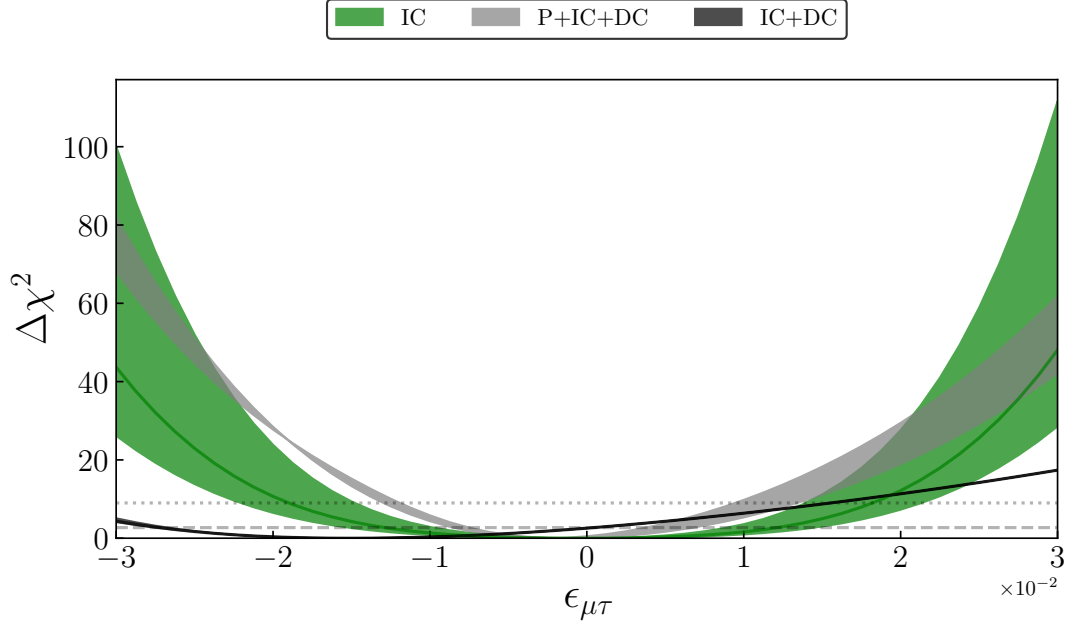

FIG. 3: $\epsilon_{\mu\tau}$ $\Delta\chi^2$ regions for scenarios as defined in Table I. Δm_{31}^2 and θ_{23} and have been marginalized out, and all other NSI parameters other than $\epsilon_{\mu\tau}$ are fixed to zero.

(a) $P_{\mu\mu}(\epsilon_{\mu\tau}^+) - P_{\mu\mu}(\epsilon_{\mu\tau}^-)$ using $\epsilon_{\mu\tau}^{\pm} = \pm0.05$ in the DeepCore/PINGU energy range.

(b) The best-fit event count ratio from each detector for $\epsilon_{\mu\tau} = \pm0.01$. IceCube only observes a small surplus of events for $\epsilon_{\mu\tau} = -0.01$ compared to DeepCore and PINGU due to the weak NSI effect at high GeV energies.
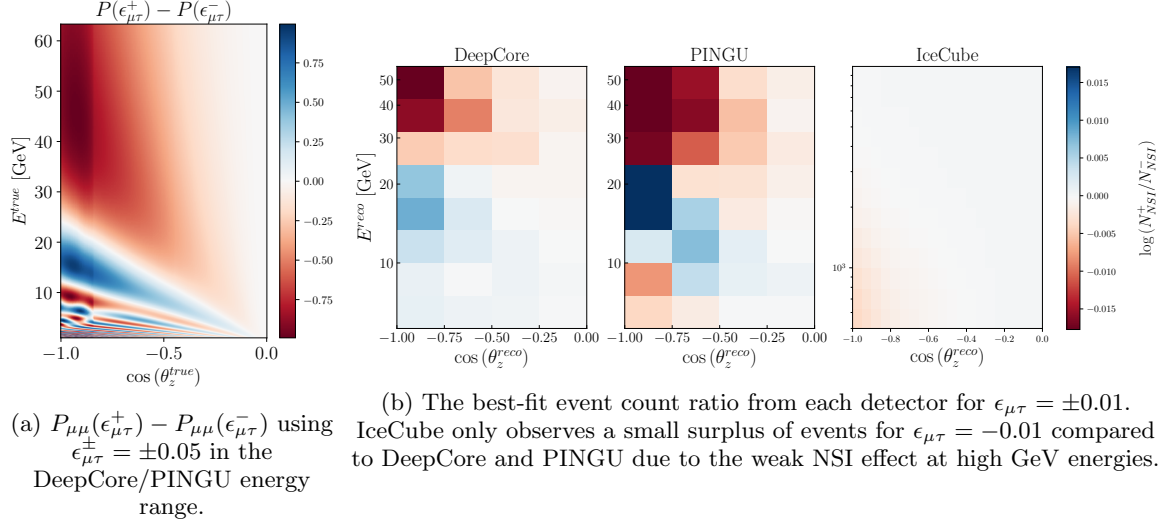
FIG. 4: Probability difference and best-fit event count. Negative $\epsilon_{\mu\tau}$ has the strongest signal, as the thin blue region stemming from $\epsilon_{\mu\tau} = 0.05$ is less prominent than the red regions from $\epsilon_{\mu\tau} = -0.05$.

Parameter	Best 90% CL	Best 3σ	Baseline 90% CL	Baseline 3σ	Worst 90% CL	Worst 3σ
			IceCube			
$\epsilon_{\mu\tau}$	[-0.01, 0.009]	[-0.015, 0.014]	[-0.013, 0.012]	[-0.019, 0.018]	[-0.015, 0.014]	[-0.022, 0.021]
			DeepCore			
$\epsilon_{\tau\tau}$	[-0.04, 0.063]	[]	[-0.04, 0.063]	[]	[-0.04, 0.063]	[]
$\epsilon_{\mu\tau}$	[-0.023, 0.007]	[0.023]	[-0.023, 0.007]	[0.023]	[-0.023, 0.007]	[0.023]
$\epsilon_{e\mu}$	[-0.107, 0.113]	[-0.198, 0.19]	[-0.107, 0.113]	[-0.198, 0.19]	[-0.107, 0.113]	[-0.198, 0.19]
$\epsilon_{e\tau}$	[-0.111, 0.212]	[-0.26, 0.3]	[-0.111, 0.212]	[-0.26, 0.3]	[-0.111, 0.212]	[-0.26, 0.3]
			IceCube + DeepCore			
$\epsilon_{\mu\tau}$	[-0.027, 0.0]	[0.016]	[-0.027, 0.0]	[0.016]	[-0.027, 0.0]	[0.016]

TABLE II: IceCube and DeepCore results from the $\Delta\chi^2$ in Fig. 3. Best, baseline, and worst refer to the systematic uncertainty scenarios considered as in Table I.

with test statistic $\chi^2_{\text{joint,min}}$. The $\Delta\chi^2_{\text{joint}}$ is then $\Delta\chi^2_{\text{joint}} = \chi^2_{\text{joint}} - \chi^2_{\text{joint,min}}$. The results are shown in Fig. ?? and summarized in Tables II and III.

Parameter	Best 90% CL	Best 3σ	Baseline 90% CL	Baseline 3σ	Worst 90% CL	Worst 3σ
			PINGU			
$\epsilon_{\tau\tau}$	[-0.033, 0.057]	[-0.048]	[-0.034, 0.059]	[-0.051]	[-0.037, 0.062]	[-0.055]
$\epsilon_{\mu\tau}$	[-0.007, 0.007]	[-0.011, 0.013]	[-0.007, 0.008]	[-0.012, 0.014]	[-0.008, 0.009]	[-0.014, 0.016]
$\epsilon_{e\mu}$	[-0.062, 0.057]	[-0.122, 0.104]	[-0.081, 0.067]	[-0.162, 0.12]	[-0.106, 0.08]	[-0.199, 0.141]
$\epsilon_{e\tau}$	[-0.07, 0.077]	[-0.12, 0.133]	[-0.086, 0.089]	[-0.15, 0.148]	[-0.107, 0.102]	[-0.182, 0.164]
			DeepCore + PINGU			
$\epsilon_{\tau\tau}$	[-0.033, 0.05]	[-0.048, 0.065]	[-0.033, 0.052]	[-0.05, 0.067]	[-0.035, 0.051]	[-0.052, 0.068]
$\epsilon_{\mu\tau}$	[-0.007, 0.006]	[-0.011, 0.012]	[-0.007, 0.006]	[-0.012, 0.012]	[-0.004, 0.011]	[-0.01, 0.017]
$\epsilon_{e\mu}$	[-0.057, 0.052]	[-0.107, 0.095]	[-0.067, 0.06]	[-0.127, 0.107]	[-0.097, 0.056]	[-0.165, 0.11]
$\epsilon_{e\tau}$	[-0.063, 0.075]	[-0.113, 0.128]	[-0.074, 0.086]	[-0.136, 0.142]	[-0.115, 0.065]	[-0.184, 0.131]
			IceCube + DeepCore + PINGU			
$\epsilon_{\mu\tau}$	[-0.009, 0.004]	[-0.013, 0.009]	[-0.009, 0.004]	[-0.014, 0.01]	[-0.008, 0.007]	[-0.012, 0.013]

TABLE III: PINGU and joint results from the $\Delta\chi^2$ in Fig. 2. Best, baseline, and worst refer to the systematic uncertainty scenarios considered as in Table I.

Parameter	Best fit		
	Δm^2_{31}	θ_{23}	ϵ
		DeepCore	
$\epsilon_{\tau\tau}$	2.435	47.84	0.0125
$\epsilon_{\mu\tau}$	2.435	43.97	-0.005
$\epsilon_{e\mu}$	2.435	43.97	0
$\epsilon_{e\tau}$	2.435	43.97	0.05
		IceCube	
$\epsilon_{\mu\tau}$	2.435	51.70	0
		IceCube + DeepCore	
$\epsilon_{\mu\tau}$	2.517	43.97	-0.01

TABLE IV: Best fit points for Δm^2_{31} and θ_{23} are given in units of 10^{-3}eV^2 and degrees, respectively.

[1] M. Honda et al., Calculation of atmospheric neutrino flux using the interaction model calibrated with atmospheric muon data.doi:10.1103/PhysRevD.75.043006.
[2] A. M. Dziewonski and D. L. Anderson, Preliminary reference Earth model 25 (4) 297–356. doi:10.1016/0031-9201(81)90046-7.
[3] M. G. Aartsen et al., Searching for eV-scale sterile neutrinos with eight years of atmospheric neutrinos at the IceCube Neutrino Telescope 102 (5) 052009. doi:10.1103/PhysRevD.102.052009.
[4] IceCube Collaboration, All-sky point-source IceCube data: Years 2010-2012. doi:10.21234/B4F04V.
[5] C. Weaver, Evidence for Astrophysical Muon Neutrinos from the Northern Sky 149.
[6] IceCube Collaboration, Search for sterile neutrinos with one year of IceCube data.
URL https://icecube.wisc.edu/data-releases/2016/06/search-for-sterile-neutrinos-with-one-year-of-icecube-data/
[7] IceCube Collaboration, Three-year high-statistics neutrino oscillation samples. doi:10.21234/ac23-ra43.
[8] IceCube Collaboration et al., Measurement of Atmospheric Neutrino Oscillations at 6–56 GeV with IceCube DeepCore 120 (7) 071801. doi:10.1103/PhysRevLett.120.071801.
[9] IceCube Collaboration 1 et al., Measurement of atmospheric tau neutrino appearance with IceCube DeepCore 99 (3) 032007. doi:10.1103/PhysRevD.99.032007.
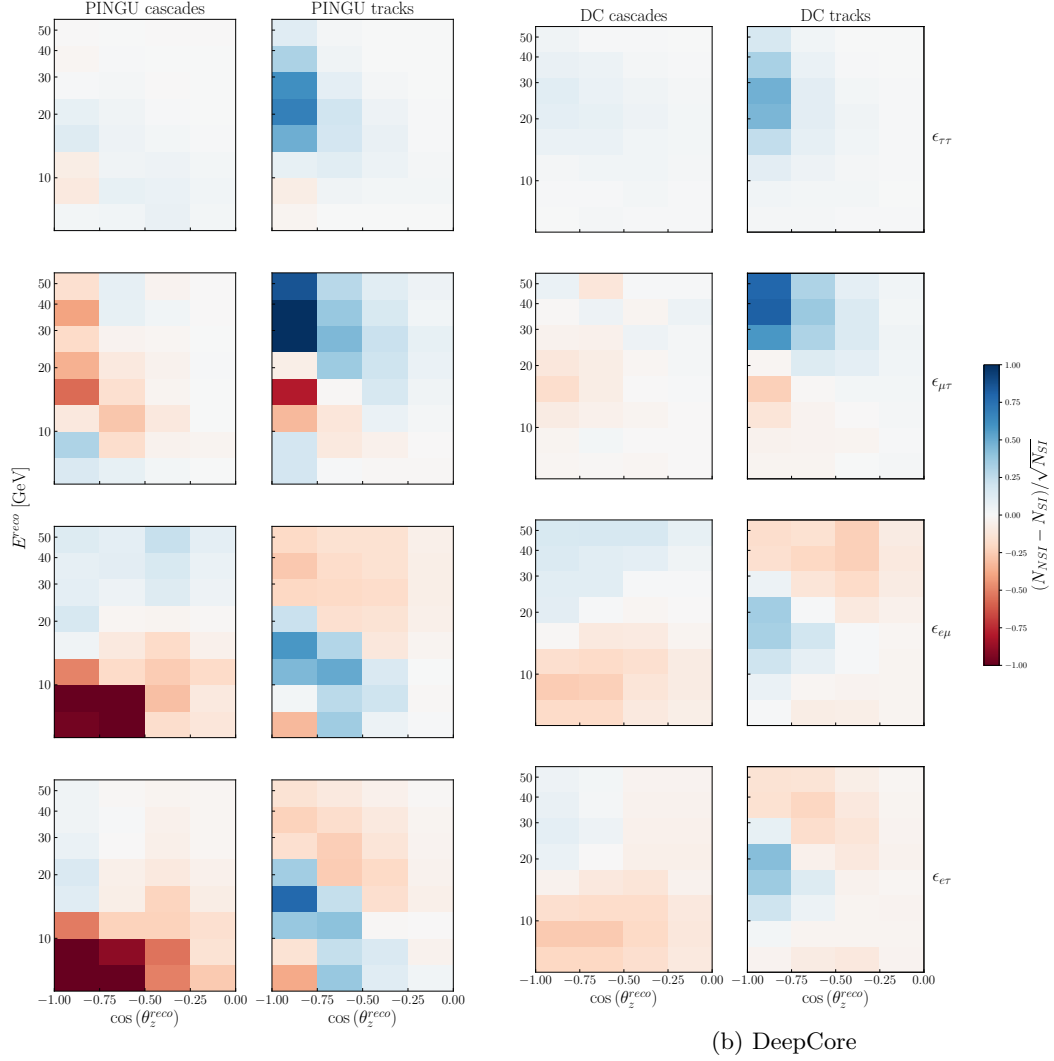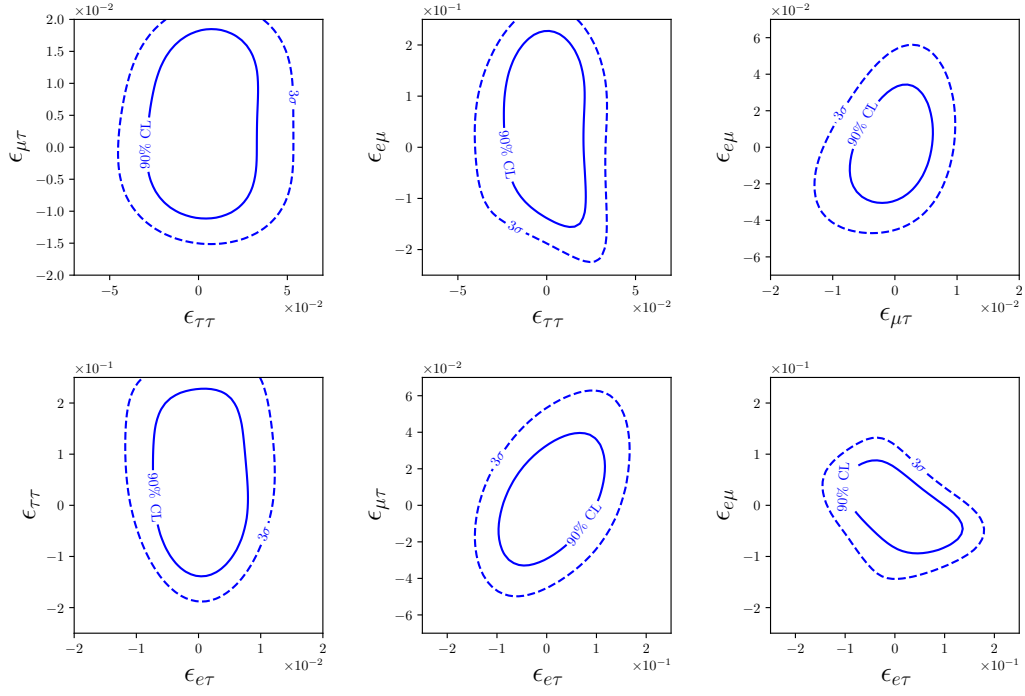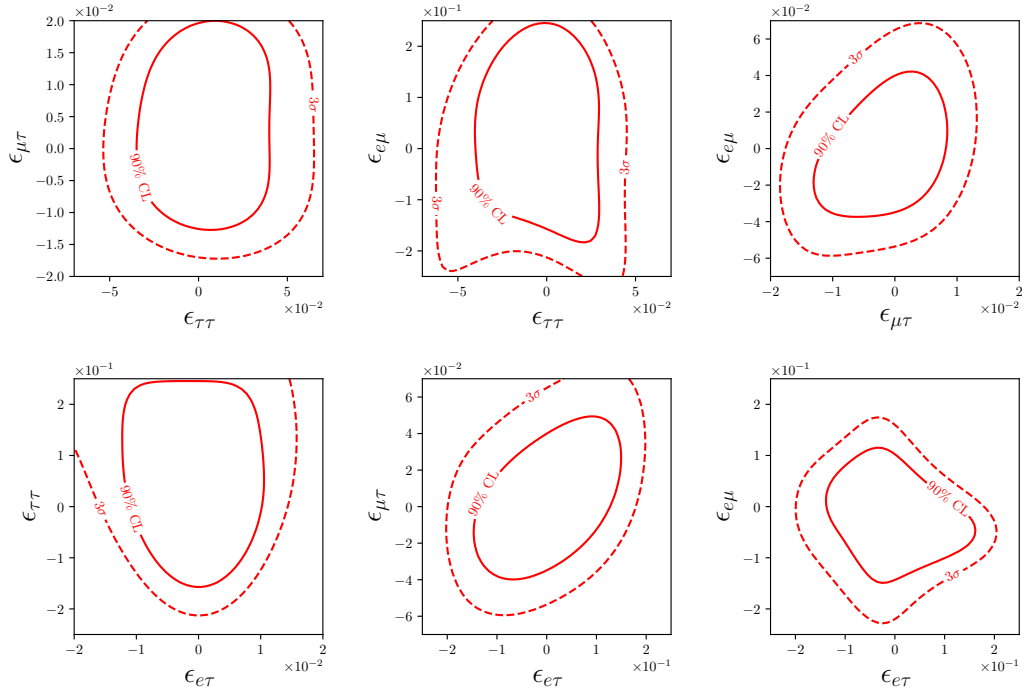
(a) PINGU

(b) DeepCore

FIG. 5: Expected pulls of the form $(N_{NSI} - N_{SI})/\sqrt{N_{SI}}$ for PINGU and DeepCore after 3 years. We compare the NSI event count with $\epsilon_{\mu\tau} = -0.01$ to the standard interaction count

[10] I. Esteban et al., The fate of hints: Updated global analysis of three-flavor neutrino oscillations 2020 (9) 178. `doi: 10.1007/JHEP09(2020)178`.

[11] IceCube Collaboration, IceCube Upgrade Neutrino Monte Carlo Simulation. `doi:10.21234/qfz1-yh02`.

[12] M. Maltoni and T. Schwetz, Testing the statistical compatibility of independent data sets 68 (3) 033020. `arXiv:hep-ph/0304176`, `doi:10.1103/PhysRevD.68.033020`.

$f = 0\%$

$f = 5\%$

DeepCore (2017)

- ✓ Honda atmospheric fluxes
- ✗ Only look at tracks and $\epsilon_{\mu\tau}$
- ✗ DC Monte Carlo from an older dataset
- ✗ 8 E bins from $6.3\,\text{eV}^2$ to $56\,\text{eV}^2$
- ✗ 8 z bins from -1 to 0
- ✗ Use "Overall" and "relative ν_e to ν_μ" normalization
- ✗ Prior on spectral index
- ✗ No zenith angle normalization
- ✓ No priors on $\Delta m^2_{31}, \theta_{23}, \theta_{13}$

Demidov (2020) DC analysis

- ✓ Honda atmospheric fluxes
- ✓ Looks at tracks + cascades for $\epsilon_{\mu\tau}$ and $\epsilon_{\tau\tau}$
- ✓ Data and Monte Carlo from DC 2018
- ✓ 8 E bins from $5.6\,\text{eV}^2$ to $56\,\text{eV}^2$
- ✓ 8 z bins from -1 to 1
- ✗ Use "Overall" and "relative ν_e to ν_μ" normalization
- ✗ Prior on spectral index
- ✗ No zenith angle normalization
- ✓ No priors on $\Delta m^2_{31}, \theta_{23}$
- ✓ Fixes $\Delta m^2_{21}, \theta_{12}, \theta_{13}$
- ✗ Uncertainty on hadron production in atmosphere
- ✗ Uncertainty on neutrino nucleon cross section

This DC+PINGU analysis

- ✓ Honda atmospheric fluxes
- ✓ Tracks and cascades for all flavors
- ✓ Reco → true mapping from Monte Carlo migration matrix
- ✓ 8 E bins from $5.6\,\text{eV}^2$ to $56\,\text{eV}^2$
- ✓ 8 zenith angle bins from -1 to 1
- ✓ Flux normalization uncertainty of 25%
- ✓ Zenith angle uncertainty of 4%
- ✓ No priors on oscillation parameters
- ✓ Marginalize Δm^2_{31} and θ_{23}. All other oscillation parameters are fixed.